

Article

Development of Transmission Systems for Parallel Hybrid Electric Vehicles

Po-Tuan Chen ^{1,2,†} , Ping-Hao Pai ^{3,†}, Cheng-Jung Yang ^{4,*} and K. David Huang ^{3,*}

¹ Center for Condensed Matter Sciences, National Taiwan University, Taipei 10617, Taiwan; r92222019@ntu.edu.tw

² Center of Atomic Initiative for New Materials, National Taiwan University, Taipei 10617, Taiwan

³ Department of Vehicle Engineering, National Taipei University of Technology, Taipei 10608, Taiwan; a8201260@yahoo.com.tw

⁴ Department of Mechanical Engineering, National Pingtung University of Science and Technology, Pingtung 91201, Taiwan

* Correspondence: cjyang@mail.npust.edu.tw (C.-J.Y.); kdavidh@ntut.edu.tw (K.D.H.); Tel.: +886-8-7703202 (ext. 7012) (C.-J.Y.); +886-2-2771-2171 (ext. 3676) (K.D.H.)

† These authors contributed equally to this work.

Received: 12 March 2019; Accepted: 10 April 2019; Published: 13 April 2019



Abstract: This study investigated the matching designs between a power integration mechanism (PIM) and transmission system for single-motor parallel hybrid electric vehicles. The optimal matching design may lead to optimal efficiency and performance in parallel hybrid vehicles. The Simulink/Simscape environment is used to model the powertrain system of parallel hybrid electric vehicles, which the characteristics of the PIM, location of the gearbox at the driveline, and design of the gear ratio of a gearbox influenced. The matching design principles for torque-coupled-type PIM (TC-PIM) parameters and the location of the gearbox are based on the speed range of the electric motor and the internal combustion engine. The parameters of the TC-PIM (i.e., k_1 and k_2) are based on the k ratio theory. Numerical simulations of an extra-urban driving cycle and acceleration tests reveal that a higher k_{ratio} has greater improved power-assist ability under a pre-transmission architecture. For example, a k_{ratio} of 1.6 can improve the power-assist ability by 8.5% when compared with a k_{ratio} of 1. By using an appropriate gear ratio and k_{ratio} , the top speed of a hybrid electric vehicle is enhanced by 9.3%.

Keywords: hybrid electric vehicle; power integration mechanism (PIM); transmission system; pre-transmission

1. Introduction

In recent years, environment-friendly vehicle technologies have been developed for solving problems that are caused by conventional vehicles. The primary purpose is to reduce emission. One of the plausible solutions is to introduce electric power into vehicles. Nowadays, powertrain technologies can be classified into pure electric power and oil-electric hybrid power types. Pure-electric power vehicles are piloted without any emissions. However, pure-electric power vehicles have some concerns, such low travel distance and long recharge time. Therefore, the performance of a battery system that provides energy to electric motor (EM) is an important issue. For instance, Samadani et al. developed a prediction model with high accuracy in both cumulative energy and the temperature of the Li-ion battery [1]. Panchal et al. proposed the electrical and thermal performance evaluation of a Li-ion battery pack in the real work drive cycle [2]. In addition, pure-electric power vehicles may not reduce emissions in some regions, because electric power generation is dependent on fossil fuel combustion.

The improvement of power storage technology [3,4] and alternative clean electric power sources [5,6] remains challenging. Therefore, oil-electric hybrid-powered electric vehicles (EVs) may be a promising solution for environment-friendly vehicles until the major challenges of pure EVs are overcome [7].

The development of hybrid vehicles comprises four challenges: research and development of a low-carbon energy carrier, system control strategy, power unit, and transmission system. Among them, the transmission system is the primary factor in integrating mechanical power and performance for hybrid vehicles. For smooth coordination between the two power outputs, the power integration mechanism (PIM) design is the most crucial for the parallel hybrid powertrain. The propulsion systems of oil-electric hybrid vehicles comprise two power units. On the basis of the power flow of power units, the power architecture of hybrid-powered vehicles can be classified into series hybrid, parallel hybrid, and series-parallel hybrid power architectures. For the series hybrid power architecture, engine power and traction power are provided to the generator and the traction motor, respectively. This architecture must include two electric machines: one with a generator and traction motor and another with an internal combustion engine (ICE). Due to the engine powering the generator, the overall efficiency of the series hybrid power architecture is generally higher than that of the parallel hybrid power architecture. However, system performance depends on the specification of the traction motor. The system performance of the series hybrid architecture is worse than that of the parallel hybrid architecture [8].

For the parallel hybrid power architecture, engine power can be used as the traction power or generator power, and the electric machine can work as a traction motor or generator depending on the system control strategy. In this system, an engine and a motor or each can provide the required traction power alone; thus, the performance of the parallel hybrid vehicles is higher than that of series hybrid vehicles. The parallel hybrid architecture can comprise an electric machine (motor/generator) and ICE [9]. Xia et al. developed a time efficient energy management strategy for the parallel plug in a hybrid electric vehicle based on the convex optimization and the simulated annealing algorithm [9]. Kim et al. evaluated the max fuel economy potential parallel hybrid electric vehicle by considering power electronics, drivetrain loss, and system loss [10]. The series-parallel hybrid power architecture combines both series and parallel systems to enhance the overall efficiency and the performance of the system. The series-parallel hybrid power architectures require two electric machines to work as the traction motor and generator. The series-parallel hybrid architecture has superior efficiency and performance, nevertheless the system is extremely complex and costly.

The hybridization factor and function of the EM can be classified into micro hybrid, mild hybrid, and strong hybrid factors and functions. The hybridization factor is a ratio that presents the percentage of EM power in a vehicle propulsion system. According to Lukic [11], the hybridization factor has a considerable effect on the performance and total efficiency of the hybrid vehicles. On the basis of the hybridization factor, the design can be classified into five types [12]. According to Miller [13], the distinct propulsion architecture for the parallel hybrid powertrain can be classified into pre-transmission and post-transmission. In the pre-transmission architecture, the mechanical power flow is first integrated and then adjusted to traction wheels (TWs) through transmission. In the post-transmission architecture, the mechanical power flow is first adjusted through transmission and is then integrated with TWs. Saiful [14] studies the differences between the performance of torque-coupled type hybrid vehicles with pre-transmission and post-transmission architectures. The result shows that the average engine efficiency slightly improved for the pre-transmission architecture; however, the overall efficiency and acceleration performance are superior for the post-transmission architecture. Hoang and Yan presented the configuration synthesis of series-parallel hybrid transmission with eight-bar mechanisms and demonstrated the feasibility [15]. Bonfiglio et al. evaluated the electrical losses and the average ICE efficiency in different operating conditions in the continuously variable transmission architecture and discontinuously variable transmission architecture [16]. Zhang [17] investigated the location and number of clutches for the hybrid powertrain of Toyota Prius and Chevrolet Volt, which are hybrid powertrains with a single planetary gear. The result shows that applying one clutch in the Toyota Prius

transmission can improve fuel consumption by 16% under the federal urban driving cycle (FUDS). Applying two clutches from Chevrolet Volt transmission can evidently improve fuel consumption, irrespective of the city or highway driving cycle.

Although various principles have been proposed, how the intriguing k ratio [18] influences the performance and efficiency of hybrid EVs has not been investigated so far. Therefore, we performed numerical simulations to examine the effect of design matching between the PIM and transmission system for single-motor parallel hybrid EVs. In this study, the Simulink/Simscape environment is used to construct a model of the parallel hybrid EV powertrain system, which PIM characteristics, locations of the gearbox at the driveline, and design of the gear ratio of the gearbox affect. This paper focuses on the influence of k_1 and k_2 , which are the design parameters for the PIM. The matching design of the torque-coupled-type PIM (TC-PIM) and the gearbox improves the efficiency and performance of parallel hybrid vehicles. The matching design principle for TC-PIM parameters and the location of the gearbox are based on the speed range of two power units. The simulation results show that the transmission system design correlates vehicle performance and it uses the combined power of two power units. The design matching principle that is proposed in this study can identify the effective design range of TC-PIM parameters and the gear ratio of the gearbox. The finding in this study can be used as a design reference theory for the transmission system of a parallel hybrid vehicle that may improve fuel consumption, irrespective of the city or highway driving cycle.

2. Materials and Methods

Section 2.1 introduces the basic theory for this study. The proposed parallel hybrid vehicle model for the transmission system and vehicle performance is based on the aforementioned theory. Section 2.2 presents the analysis of the transmission design for parallel hybrid vehicles. Section 2.3 focuses on the transmission design of the TC-PIM. The details of nomenclatures that are discussed in this section are also listed in the section of Appendix A.

2.1. Basic Theory

2.1.1. Vehicle Longitudinal Dynamic

We briefly quote the basic theory vehicle longitudinal dynamic from Ref. [19]. When the vehicle is being driven, sufficient traction force is required to move the vehicle. By using a transmission transit suitable torque to TWs, the power unit provides the traction force, which can be expressed using Equation (1).

$$F_T = \frac{T_w}{r_{weff}}. \quad (1)$$

To simplify the analysis process, the demand traction force can be determined while using the total resistance when driving, which can be expressed using Equation (2).

$$F_T = F_R + F_D + F_G. \quad (2)$$

The driving resistance in longitudinal motion comprises tire rolling resistance, drag resistance, and grade resistance. The deformation of the load on the tire when the tire is rolling on the road surface causes the tire rolling resistance. Therefore, the actual tire radius becomes smaller than the nominal dimension when rolling. When the tire starts rolling, the reaction force of the normal force is applied on a tiny offset from the tire center due to hysteresis. Therefore, the reaction force generates a reaction moment on the tire. If the reaction moment is equivalent to the force that is applied on the contact point of the tire and road surface, the tire rolling resistance can be expressed using Equation (3).

$$F_R = f_R \cdot N = \frac{d}{r_{weff}} N. \quad (3)$$

The actual rolling resistance coefficient of the tire is influenced by the dimension and compound of the tire, camber angle, vehicle speed, and road friction. To simplify the analysis, the road friction is only considered to influence the tire rolling resistance coefficient; thus, Equation (3) can be simplified using Equation (4).

$$F_R = f_R \cdot mg \cdot \cos \theta. \quad (4)$$

In general, the rolling resistance coefficient of the road is in the range of 0.01–0.05. In this study, the rolling resistance coefficient of 0.02 was used for a common asphalt road.

Air resistance causes the drag resistance. When the vehicle is being driven, the vehicle body moves through air in front of the vehicle. In this motion, air provides a force that moves along the vehicle body. This force changes the streamline velocity of air; thus, the turbulence zone is formed behind the vehicle body. As the turbulence zone has a pressure difference with normal air, this pressure difference generates resistance for vehicle movement, which is called drag resistance. The value of drag resistance is related to the vehicle driving speed, drag coefficient, and front area of the vehicle body. The drag resistance can be expressed using Equation (5).

$$F_D = \frac{1}{2} \cdot \rho \cdot C_d \cdot A \cdot v^2 \quad (5)$$

The grade resistance is caused by the gravity of the vehicle. Due to the slope of the road, a part of the gravitational force acts in the downhill direction. This force can be expressed using Equation (6).

$$F_G = mg \cdot \sin \theta \quad (6)$$

According to Newton's second law, the acceleration of an object in linear motion can be expressed using Equation (7).

$$F = m \cdot a \quad (7)$$

Therefore, if the traction force minus all of the resistances mentioned above also exceeds zero, it can provide the acceleration force for vehicles, which can be expressed using Equation (8).

$$F_t - (F_R + F_D + F_G) = (m + m^*) \cdot a \quad (8)$$

The notation m^* indicates the added mass of rotating components because of rotating motion. The maximum vehicle speed can be calculated using the traction force and power of the power unit. In general, the maximum vehicle speed is discussed at level ground ($\theta = 0$) and, thus, the maximum vehicle speed can be expressed using Equation (9), as follows:

$$V_{max} = \frac{(F_R + F_D)}{P_{max}} \quad (9)$$

2.1.2. Transmission Design Demand

The transmission system is the most critical system design for vehicle performance. The primary aim of the vehicle transmission system is to maintain power units to provide suitable traction power under various working conditions. Thus, the power units are always operating under high efficiency. Therefore, if a vehicle has a suitable transmission system, then it has reduced fuel consumption and emission. Fischer [18] reveals that the vehicle transmission design must satisfy two primary demands: providing the required traction force under various driving conditions for favorable vehicle performance and operating power units under high efficiency to reduce fuel consumption and emission. However, these primary design demands are contradictory in some models. To design a suitable transmission system, the optimal matching of the power unit is required for efficient fuel consumption and favorable vehicle performance. The key factors are (i) the traction force that is required by

calculating the total resistance, which is applied on the vehicle body [18] and (ii) the gear ratio design for the driving power unit operating at the highest efficiency [20].

2.1.3. Power Integration Mechanism

The PIM is a crucial component in the hybrid propulsion system. The function of the PIM is to integrate input mechanical power from two independent sources into output mechanical power within its constraints. Figure 1 shows that the PIM is a two-degree-of-freedom mechanism and it has at least three ports. Each port is bidirectional and it transmits mechanical power. Without any loss of efficiency, the in-flowing mechanical power is equivalent to mechanical power flow-out. For example, if ports 1 and 2 provide mechanical power, and port 3 is connected to the output shaft, then the output shaft mechanical power can be expressed using Equation (10).

$$T_3\omega_3 = T_1\omega_1 + T_2\omega_2 \tag{10}$$

Ehsani [21] classified the PIM into two types, namely torque-coupled and speed-coupled types, based on the PIM characteristics. The basic theorem of these PIMs is described, as follows:

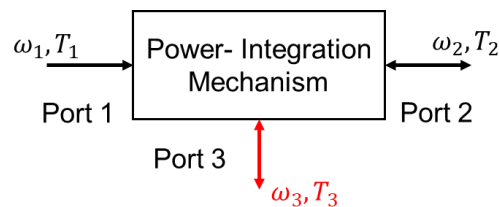


Figure 1. Power integration mechanism.

The characteristic of the TC-PIM is that the output torque demand can be satisfied through the linear superposition of two independent input torques with coefficient k , which is determined while using the geometric structure of the PIM. By dividing Equation (10) by output angular velocity ω_3 , the relationship of torque for each port can be expressed using Equation (11).

$$T_3 = T_1k_1 + T_2k_2 \tag{11}$$

Equation (11) shows that the demand torque T_3 comprises T_1k_1 and T_2k_2 . Therefore, T_1 and T_2 can independently control the demand torque T_3 . The angular velocity of each port cannot be independently controlled because of the power conservation constraint. The angular velocity constraint can be expressed using Equation (12).

$$\omega_3 = \frac{\omega_1}{k_1} = \frac{\omega_2}{k_2} \tag{12}$$

The characteristic of the speed-coupled PIM is that the output speed demand can be satisfied through the linear superposition of two independent input speeds divided by coefficient k , which is determined while using the geometric structure of the PIM. By dividing Equation (10) by output angular velocity ω_3 , the relationship of speed for each port can be expressed using Equation (13).

$$\omega_3 = \frac{\omega_1}{k_1} + \frac{\omega_2}{k_2} \tag{13}$$

Equation (13) shows that the demand speed ω_3 comprises ω_1/k_1 and ω_2/k_2 . Thus, ω_1 and ω_2 can independently control the demand speed ω_3 . The torque of each port cannot be independently controlled due to the power conservation constraint. The torque constraint can be expressed using Equation (14).

$$T_3 = k_1T_1 = k_2T_2 \tag{14}$$

2.1.4. Driving Mode Control Architecture

The driving mode control architecture is important in the parallel hybrid propulsion system. In general, the hybrid vehicle has five primary driving modes, namely EV mode, ICE mode, power-split mode, hybrid mode, and regenerate brake mode. The control rule to switch the driving modes in this study is based on demand power classification. Lin [22] presents the demand power classification for driving mode switch logic for hybrid trucks. In demand power classification, constant power lines are used to separate the engine power into three operation regions. These regions can be classified into low-, medium-, and high-power regions. As the engine has superior efficiency in the medium power region, motor in low power demand and engine and motor in high power demand. By using this approach, fuel consumption can be reduced, and driving mode control rule can be established.

2.2. Parallel Hybrid Transmission Design

The specification of engine and motor and the parameters in this section for following numerical simulations were obtained from Matlab Simulink of ADVISOR®Software (MathWorks Inc.: Natick, MA, USA, 2018) and Advanced Vehicle Simulator [23].

2.2.1. Specification of Power Units

The data include power specification and efficiency data. Therefore, the data can be used to determine the traction force and energy usage for the hybrid propulsion system. A 1.0L spark-ignition (SI) engine, which can provide 41 kW power and 81 Nm torque at peak performance, is used. Table 1 provides the details. A permanent magnet direct current (PMDC) motor, which can provide a power of 10 kW and a torque of 46.5 Nm for the peak values, is used as the EM/generator. Figure 2b shows the efficiency map of this motor, where the thick black line is the motor power envelope. The negative phase of the torque indicates that the motor works as a generator; thus, the efficiency contour in this phase indicates the recharge efficiency. In the hybrid mode, the operating region of the power unit has some system constraints and, thus, it cannot freely operate power units. Figure 2a shows the brake specific fuel consumption map of this engine, where the thick black line represents the engine power envelope under the wide-open throttle condition.

Table 1. Engine specification.

	Geo Metro 1.0L SI engine	10 kW PMDC Motor
Peak power	41 kW/5700 rpm	10 kW
Peak torque	80.9 Nm/3477 rpm	46.5 Nm
Speed range	1000–6000 rpm	0–8500 rpm
Voltage	n/a	60 V
Max Current	n/a	180 A

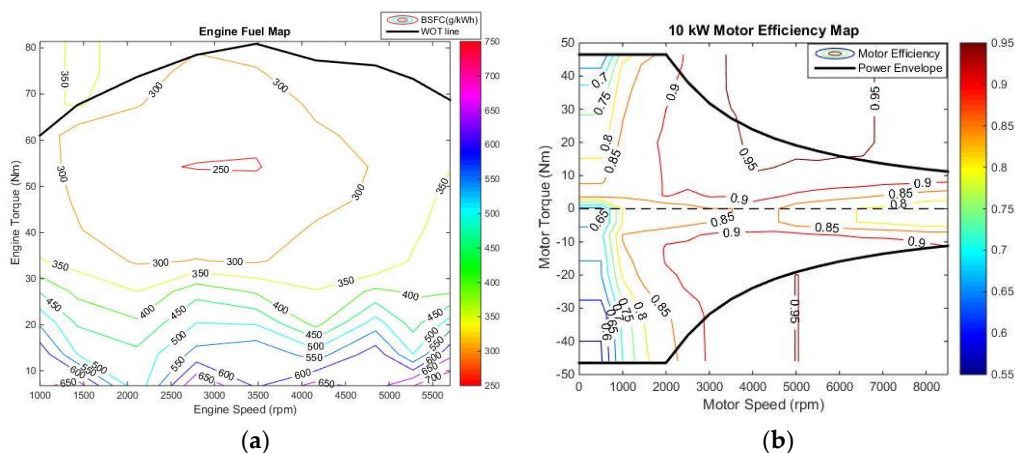


Figure 2. (a) Engine map and (b) electric motor (EM) map.

2.2.2. Transmission Design Requirements

Speed is a crucial factor in forces on driving vehicles. Table 2 shows the design requirement of transmission and the parameters of the driving vehicle. These values were obtained from Matlab Simulink of ADVISOR® Software and Advanced Vehicle Simulator [23].

Table 2. Design requirement of transmission and corresponding parameters.

Design Demand	Value
Maximum traction force of tire	3500 N
Maximum slope at 10 km/h	25%
Top vehicle speed	ICE: 161 km/h Hybrid: 176 km/h
Engine max stat rpm	3000 rpm
Motor max power in EV mode	8.5 kW
Engine max power in ICE mode	25 kW
φ_2	1.1
Vehicle Parameters	Value
Weight	1200 kg
Effective radius of traction wheel	0.3 m
Front area	2.16 m ²
Drag coefficient	0.26
Rolling resistance coefficient	0.02
Maximum grade resistance	2855.1 N
Rolling resistance	288.41 N
Drag resistance	2.6042 N

2.2.3. Influence of Location of Gearbox

For the parallel hybrid propulsion system, the transmission system can be placed at three locations. Figure 3 shows the possible locations of the gearbox (GB) with respect to the ICE, EM, TW, and PIM in the parallel hybrid propulsion system. These different locations of the gearbox have different effects on the torque and the rotation speed between the PIM in the hybrid driving or power-split mode. The details of the effect of each location of the gearbox are as follows:

- The influence of GB1: The torque and rotation speed of engine outputs can be independently adjusted.
- The influence of GB2: The torque and rotation speed of motor outputs can be independently adjusted.
- The Influence of GB3: The torque and rotation speed of PIM outputs can be adjusted, which indicates that the outputs of the engine and motor are simultaneously adjusted. This location of the gearbox alone cannot be used to adjust engine or motor outputs.

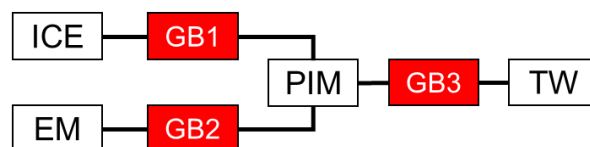


Figure 3. Gearbox location of parallel hybrid driveline.

The TC-PIM that was in this study used a spur gear train to design and analyze the parallel hybrid transmission system. Spur gears are widely used in power transmission mechanisms. It is a simple mechanism to transfer mechanical power. The theory of spur gear-type transmission is that a gear set comprises drive and driven gears. These gears have different dimensions and, thus, it can adjust the

torque and rotation speed. Equations (15) and (16) can express the relationship of the torque value and rotation speed value for drive and driven gears. The term $\frac{r_{dn}}{r_d}$ represents the gear ratio.

$$\eta \cdot \frac{T_{dn}}{T_d} = \eta \cdot \frac{r_{dn}}{r_d} \tag{15}$$

$$\frac{\omega_d}{\omega_{dn}} = \frac{r_{dn}}{r_d} \tag{16}$$

2.2.4. Torque-Coupled-Type Transmission

The aforementioned discussion examined the constraint of the TC-PIM. In this study, we select the spur gear for the TC-PIM. The following section discusses the design torque-coupled-type transmission based on speed-torque. The TC-PIM in this study uses the spur gear train to design and analyze the parallel hybrid transmission system. Spur gears are widely used in power transmission mechanisms. It is a simple mechanism that is used to transfer mechanical power. In spur gear-type transmission, a gear set comprises drive and driven gears. These gears have different dimensions and, thus, it can adjust torque and rotation speed. The relationship between the torque value and rotation speed value for drive and driven gears can be expressed using Equations (15) and (16). The term $\frac{r_{dn}}{r_d}$ also represents the gear ratio.

Figure 4a shows the basic driveline architecture for TC-PIM. In this architecture, the engine and motor are always connected with the TC-PIM, which indicates that each power unit cannot only provide power for the traction vehicle. To ensure that all of the driving modes can work, clutches or brakes must be installed in the driveline architecture. For the ICE mode and the smooth integration of mechanical power in the hybrid mode, a clutch must be installed between the EM and TC-PIM. To reduce the engine pumping loss, the clutch that is installed between the engine and TC-PIM is necessary. Figure 4b shows the suitable clutches that were added in the driveline architecture for the TC-type parallel hybrid powertrain. A brake should not be installed in driveline, as the TC-PIM is one-degree-of-freedom mechanism. When the brake is installed in the driveline, it locks up all shafts; thus, the transfer of mechanical power to the TW becomes difficult.

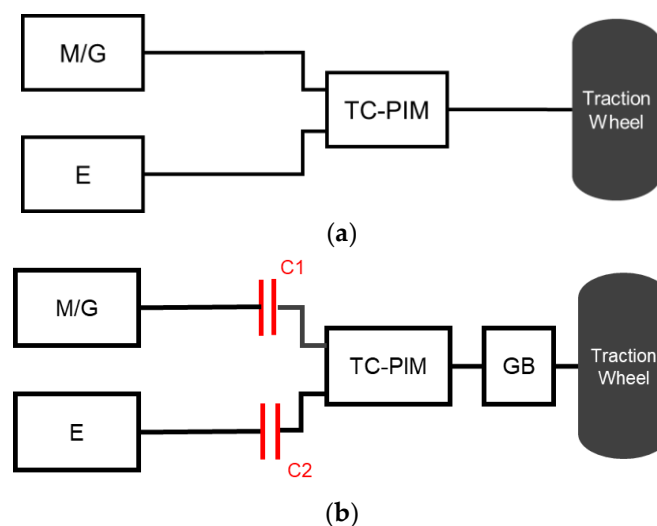


Figure 4. (a) Basic driveline architecture for the torque-coupled-type PIM (TC-PIM). (b) Clutches added driveline architecture for TC-PIM.

In the parallel hybrid mode, the gearbox can be installed at three positions. To determine the position for the installation of the gearbox, the relationship between the speed-torque characteristic of power units and the constraints of the TC-PIM must be determined [18]. The TC-PIM would restrict

the angular speed when power is integrated. The speed relationship with power units and the TC-PIM can be expressed using Equation (17), as follows:

$$\eta_{speed} = \frac{k_1 \omega_{E-max}}{k_2 \omega_{ICE-max}} \tag{17}$$

If $\eta_{speed} \ll 1$, the gearbox or single gear must be installed between the engine and TC-PIM to ensure that the engine delivers complete power (GB1). If $\eta_{speed} \gg 1$, the gearbox or single gear can be installed between the EM and TC-PIM to ensure that the EM delivers complete power (GB2). If $\eta_{speed} \cong 1$, only the gearbox must be installed behind the TC-PIM and, thus, it can simplify system complexity (GB3). Therefore, the proper placement of gearbox for this primary simulation is behind TC-PIM.

Hybrid vehicles have three driving modes, namely EV mode, ICE mode, and hybrid power mode. To satisfy all of the driving modes for satisfactory performance, the gear ratio design must consider the requirements of each driving mode. Equation (17) can be used to calculate η_{speed} , which influences the gearbox location. Therefore, the first step in designing the gear ratio is to determine the k_1 and k_2 of the TC-PIM. To ensure that all of the power units can provide power within an adequate speed range. The relationship between k_1 and k_2 , and power units with a capable speed can be obtained using the following Equation (18):

$$\omega_{3-Pmax} = \frac{\omega_{2-Pmax}}{k_2} = \frac{\omega_{1-Pmax}}{k_1} \tag{18}$$

ω_{1-Pmax} and ω_{2-Pmax} are compared to determine which term has a smaller value. The smaller term is determined for $k = 1$ and, thus, the theoretical value of k for another term can be obtained. For example, $\omega_{1-Pmax} = 5700$ and $\omega_{2-Pmax} = 8500$ are obtained for the maximum engine speed and maximum EM speed from Table 1 and then substituted into Equation (18):

$$\omega_{3-Pmax} = \frac{8500}{k_2} = \frac{5700}{1} \tag{19}$$

Thus, the maximum output power of the TC-PIM can be obtained for the hybrid driving mode, and all of the power units are operated in the capable speed range. This method is called the basic speed limit method.

$$k_{ratio} = \frac{k_2}{k_1} \tag{20}$$

In Equation (20), the k_{ratio} values can be proportionally changed for specific design requirements. If the k_{ratio} is used with a wrong design, the total integral power decreases. Moreover, the ideal maximum k_{ratio} can be expressed as Equation (21).

$$k_{ratio_max} = \frac{\omega_{2-Pmax}}{\omega_{1-Pmax}} \tag{21}$$

Equations (17)–(21) show that the appropriate k_2 value is between 1 and 1.4912 for the complete power usage of power units. On the basis of the engine map and the motor map, Figure 5a–d show the possible power regions for different k_{ratio} , that is, $k_1 = k_2 = 1$ to $k_1 = 1$ and $k_2 = 1.6$ conditions for the TC-type parallel hybrid propulsion system. The ideal maximum total power of 51 kW is summed by ICE peak power of 41 kW and electric motor of 10 kW, as in Table 1. For $k_2 = 1.6$, the maximum total power (50.4712 kW) is less than the ideal value (51 kW), because the engine cannot provide maximum power in the hybrid mode. Due to the TC-PIM being constrained by the speed relationship, the maximum speed of the motor for TC-PIM is less than 5700 rpm at $k_2 = 1.6$.

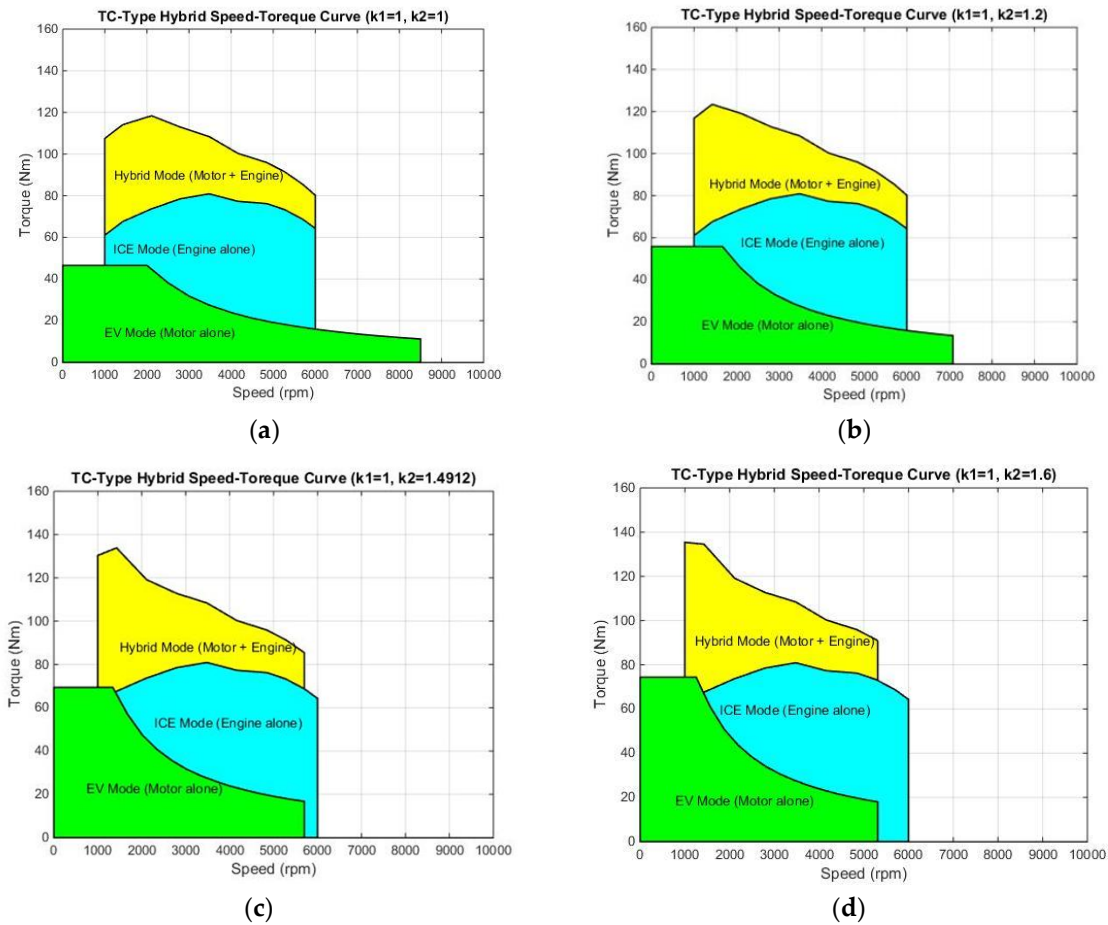


Figure 5. (a) Power region ($k_1 = 1, k_2 = 1$). (b) Power region ($k_1 = 1, k_2 = 1.2$). (c) Power region ($k_1 = 1, k_2 = 1.4912$). (d) Power region ($k_1 = 1, k_2 = 1.6$).

The first step is to determine the gear ratio in the EV mode. The second step is to determine the overall gear ratio. The overall gear ratio must be determined stepwise for all driving modes due to the different parallel hybrid driving modes. The largest gear ratio in the EV mode can be expressed using Equation (22).

$$i_{EV} = \frac{r_{weff} \cdot (F_{Gmax} + F_R + F_D)}{k_2 T_{Emax}} \tag{22}$$

Substituted parameters in Tables 1 and 2 into Equation (22) can determine $i_{EV_largest}$:

$$i_{EV} = \frac{0.3 \cdot (2855.1 + 288.41 + 2.6042)}{1.4167 \cdot 46.5} = 14.06 \tag{23}$$

The number of gears for EV mode transmission can be designed using a single gear because the EM has constant power characteristics.

The third step is to determine the overall gear ratio in the ICE mode and hybrid mode. As the engine provides the primary power to the propulsion system, and the EM just provides start-stop and power assistance; the gear ratio is mainly designed for the engine with one extra gear for hybrid power. Thus, the overall gear ratio in the ICE mode and hybrid mode can be obtained. The largest gear ratio in the ICE and hybrid mode can be expressed using Equation (24).

$$i_{ICE_largest} = \frac{r_{weff} \cdot (F_{Gmax} + F_R + F_D)}{k_1 T_{ICEmax}} \tag{24}$$

$i_{ICE_largest}$ can be determined by substituting parameters in Tables 1 and 2 into Equation (24):

$$i_{ICE_largest} = \frac{0.3 \cdot (2855.1 + 288.41 + 2.6042)}{1.80.9} = 11.67 \tag{25}$$

The fourth step is to determine the smallest gear ratio in the ICE mode and the hybrid mode. In this study, a V_{max} optima design is used to determine the smallest gear base on the ICE design and to add one more gear for excess hybrid power, which can be expressed using Equation (26).

$$i_{ICE_smallest} = 3.6 \cdot \frac{\frac{\pi}{30} \cdot r_{weff} \cdot n_{max}}{V_{max}} \tag{26}$$

$i_{ICE_smallest}$ can be determined by substituting parameters in Tables 1 and 2 into Equation (26):

$$i_{ICE_smallest} = 3.6 \cdot \frac{\frac{\pi}{30} \cdot 0.3 \cdot 5700}{161} = 4.02 \tag{27}$$

$$i_{hy-smallest} = 3.6 \cdot \frac{\frac{\pi}{30} \cdot 0.3 \cdot 5700}{176} = 3.67 \tag{28}$$

The fifth step is to determine the intermediate gear ratio by using the progressive gear steps method at $\varphi_2 = 1.1$. Table 3 shows all of the gear ratios. Figure 6 shows a traction force diagram with the designed gear ratio. The red lines indicate the total resistance under different slope and speed conditions, from bottom to top: 0% slope, 3% slope, 5% slope, 10% slope, 15% slope, 20% slope, and 25% slope. A blue line represents the motor traction force in the EV mode, and it can overcome the resistance of 25% slope at 10 km/h. Black lines represent the engine traction force with different gear ratios, from the top to bottom: first gear to fourth gear and top speed gear. With these designed gear ratios, the vehicle can reach a speed of approximately 160 and 170 km/h by using the engine and the hybrid mode, respectively.

2.3. Parallel Hybrid Vehicle Model for numerical simulation

In this section, the basic theory from Sections 2.1 and 2.2 is used to design the complete parallel hybrid vehicle propulsion systems with single EMs in the Simscape environment. This system model includes the driving control, power units, transmission architectures, and vehicle body.

Table 3. Gear ratio design values.

	Different k_{ratio}			
k_1	1	1	1	1
k_2	1.6	1.4912	1.2	1
EV	12.45	13.36	16.6	19.92
	Other parameters			
φ_1	1.298			
1st gear	11.67			
2nd gear	7.44			
3rd gear	5.21			
4th gear	4.01			
Top speed gear	3.67			

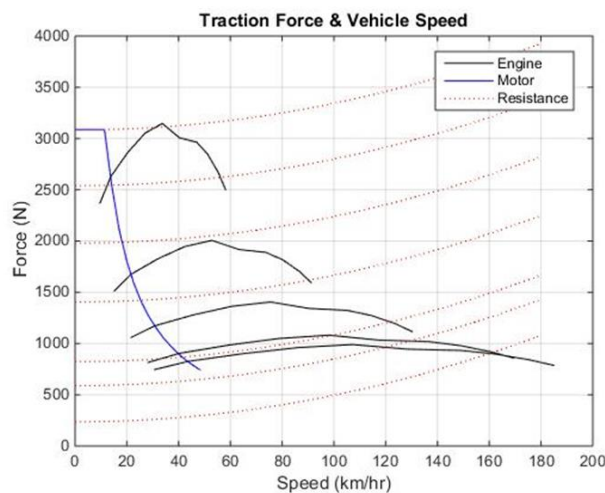


Figure 6. Traction force diagram with designed gear ratio.

2.3.1. Introduction of Simscape Environment

The basic theory from Sections 2.1 and 2.2 is used to design the complete parallel hybrid vehicle propulsion systems with single EMs in the Simscape environment [24]. This system model includes the driving control, power units, transmission architectures, and vehicle body.

Simscape is a set of block libraries and particular simulation features for modeling the physical systems in the Simulink environment [24]. It employs the physical network approach, which differs from the standard Simulink modeling approach, and it is particularly suited to simulate systems comprising real physical components. The physical network approach, with Through and Across variables and nondirectional physical connections, automatically resolves all conventional concerns with various factors, such as variables and directionality. Simscape can create a network representation of the designed system that is based on the physical network approach. According to this approach, each system comprises functional elements that interact with each other by exchanging energy through their ports. The number of connection ports for each element is determined while using the number of energy flows that were exchanged with other elements in the system, and it depends on the level of idealization. Energy flow is characterized using its variables. Each energy flow is associated with two variables, namely Through and Across. In general, and the product of these variables provides energy flow in watts.

Simscape blocks may have the following types of ports:

- Physical conserving ports—Nondirectional ports that represent physical connections and relate physical variables based on the physical network approach.
- Physical signal ports—Unidirectional ports transferring signals that use an internal Simscape engine for computations.

Physical Network approach supports the following two of variables:

- Through—Variables that are measured with a gauge connected in series with an element.
- Across—Variables that are measured with a gauge connected in parallel with an element.

To simulate and analyze the propulsion system of the hybrid EV, this study focused on electrical, mechanical rotational, and mechanical translational domain. All of the simulation was performed using the commercial program of Matlab [25].

2.3.2. Subsystem Models

Engine: The hybrid propulsion system comprises two power units of ICE and the EM, as well as containing PIM, transmission, and vehicle body. This model uses a programmed relationship between the torque and speed modulated using a throttle signal [25]. Figure 7 shows the subsystem of the engine model.

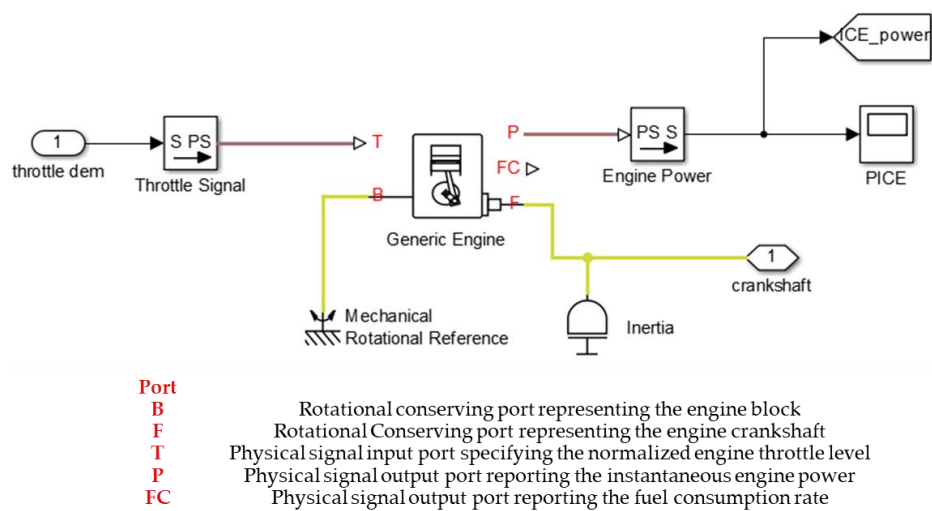


Figure 7. Engine system model.

Electric Motor: The EM model is a brushless motor model with a closed-loop torque control. This model abstracts the torque–speed behavior of the combined motor and motor driver to support system-level simulation, where simulation speed is crucial [24], and it sets the maximum torque and maximum power to obtain the torque–speed envelope, as shown in Figure 8a. Figure 8b shows the complete subsystem of the EM model and each port.

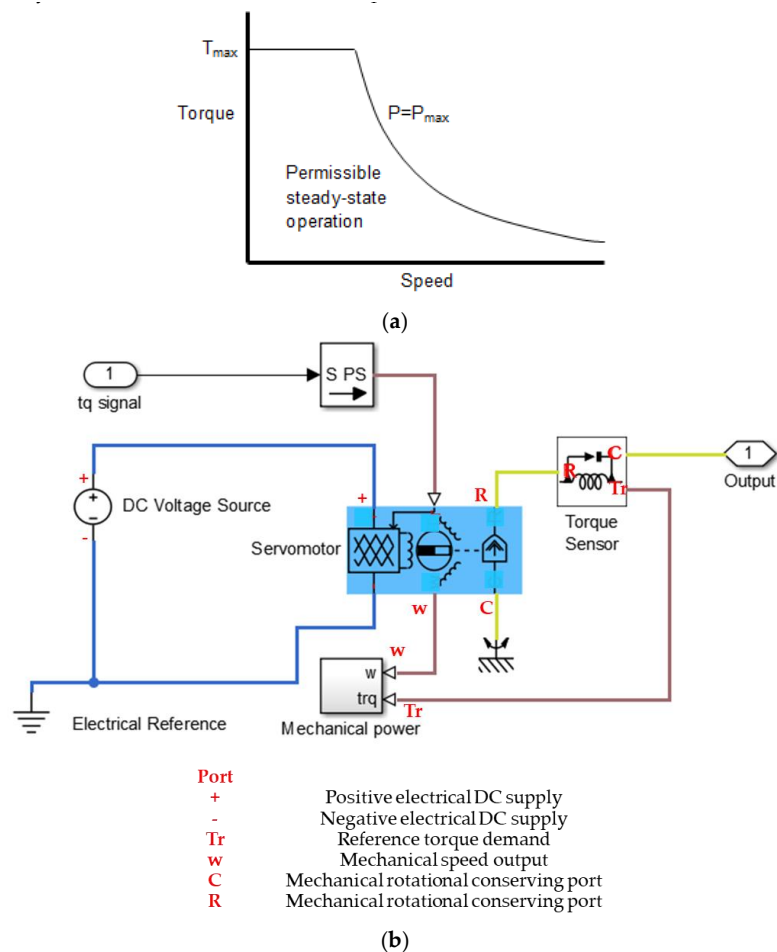


Figure 8. (a) Torque–speed envelope in motor model. (b) EM system model.

Transmission: The transmission model comprises a clutch model and gear model to simulate multigear transmission behavior. Two types of gear models can be used for the transmission model. The spur gear model with a gearbox or a TC-PIM constrains the two connected driveline axes within a fixed gear ratio and it imposes a kinematic constraint on the two connected axes using Equation (16). The torque transfer function of this model is obtained using Equation (29).

$$G_{FB}T_B + T_F - T_{loss} = 0 \tag{29}$$

In real-time applications, the angular velocity of a pair of the spur gear set exhibits an opposite rotation direction. In this study, all of the angular speeds through the spur gear set are set-up in the same rotation direction without losses to simplify the simulation process and the complexity of system model under ideal conditions. Figure 9 shows the details of a six-speed gearbox model the meaning of each port, which shifts the gear by using a controlled shift link in each clutch. Table 4 shows the clutch schedule for each gear.

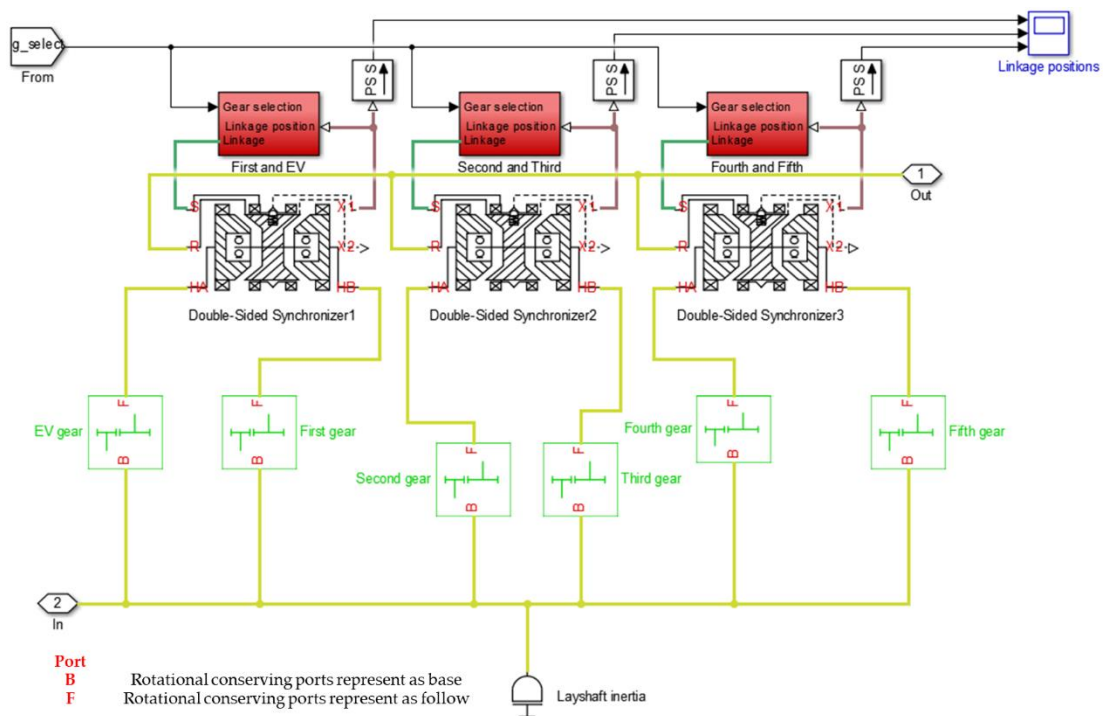


Figure 9. Gearbox system model.

Table 4. Clutch schedule.

	Clutch 1	Clutch 2	Clutch 3
EV gear	Left engaged	N	N
1st gear	Right engaged	N	N
2nd gear	N	Left engaged	N
3rd gear	N	Right engaged	N
4th gear	N	N	Left engaged
Hybrid top speed gear	N	N	Right engaged

Vehicle body: The vehicle body model includes the TWs, vehicle body, and brake system, as shown in Figure 10. The values in Table 5 are the preset recommended values that are provided by Simscape [24]. As our simulation specifications are general, the simulation is done with the recommended values that are provided in the software. Cg is the mass center of vehicles. The position of the center is related to the height of the vehicle from the ground and the position of the front and

rear axles. In this model, the slope of the road and wind velocity can be set to simulate the different conditions of the driving resistance if required. In general, there are three types of air resistance: the first is the resistance caused by the air impact on the front of the vehicle, the second is the friction resistance, and the third is the external resistance. The value of the wind velocity is also preset in Simscape.

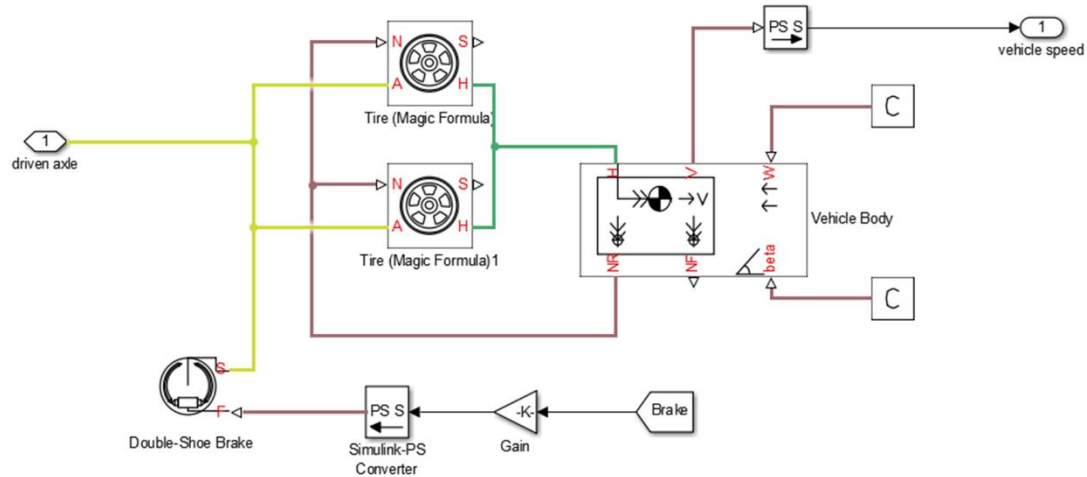


Figure 10. Vehicle body system model and parameters.

Table 5. Vehicle body parameters.

Parameter	Value
Vehicle gross weight	1200 kg
Horizon distance from Cg to front axle	1.35 m
Horizon distance from Cg to rear axle	1.35 m
Cg height above ground	0.5 m
Front area	2.16 m ²
Drag coefficient	0.26
Effective radius of tire	0.3 m
Rolling resistance coefficient	0.02

2.3.3. System Control

The system control architecture is a two-level proportional–integral–derivative (PID) control. The top level is to control the vehicle speed to the driving mode control rule is based on demand power classification. When a vehicle is started, it is driven in the EV mode. Until the speed of the shaft, which is placed before the gearbox, reaches 3000 rpm, the driving mode is changed to transfer mode 1. In this driving mode, the engine and motor are simultaneously operated until the motor torque is less than or equal to zero, and the driving mode is changed to the ICE mode. The ICE mode has two process directions. In the first direction, the ICE is changed to the EV mode when the speed is less than 2500 rpm, whereas, in the second direction, the ICE is changed to transfer mode 2 when power is higher than 25 kW. Due to the engine map showing that the superior brake-specific fuel consumption region is between 15 and 25 kW, the control strategy proposes that the constrained engine should operate in this region, thus improving the engine operating efficiency. When the value of rotating speed of motor divide k_2 greater or equal to ICE, the driving mode is changed to the hybrid mode. In this driving mode, the motor has a power-assist function and provides additional torque and, thus, the engine can operate in the smaller torque region to reduce fuel consumption. Figure 11a shows the flow chart of the driving mode control. The control of gear shifting is based on the rotational speed of power units. In addition to the EV gear, other gears are designed for the engine, and the engine map shows that the superior efficiency region of the engine is between 3000 and 5000 rpm. The shifting up and shifting

down references are higher than 5000 rpm and less than 3000 rpm, respectively. Figure 11b shows the flow chart of the gear shifting control.

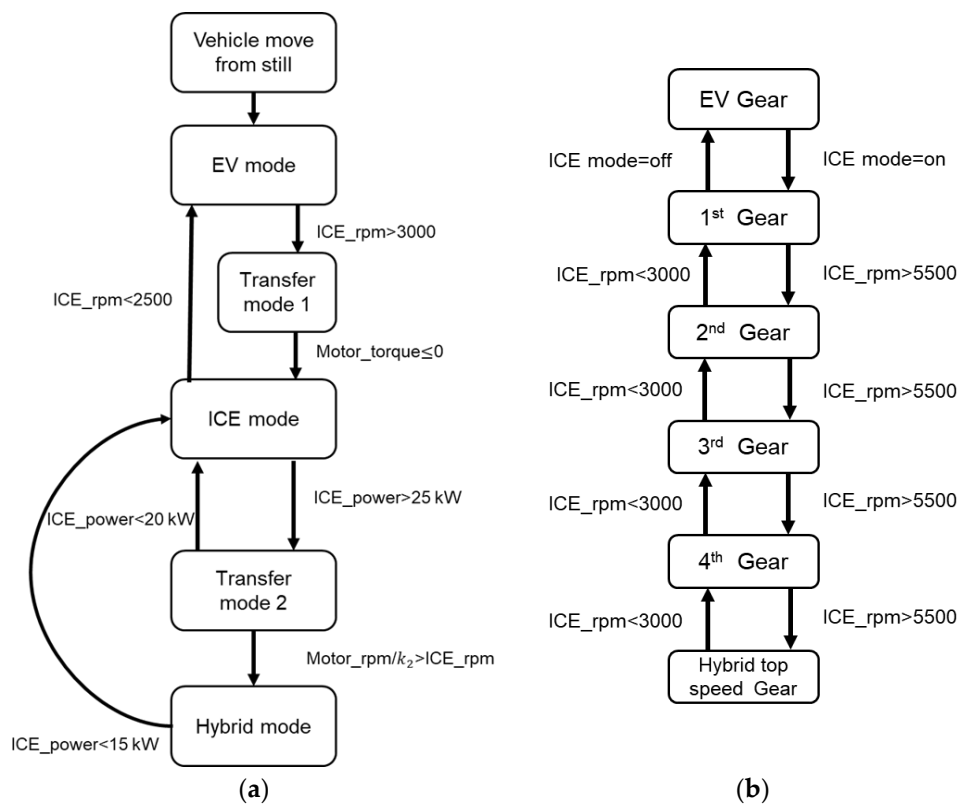


Figure 11. (a) Driving mode control logic. (b) Gear shifting control logic.

3. Results

In this section, we propose a novel transmission design that is based on the aforementioned models, and we describe with the simulation results. The simulations are performed under the extra-urban driving cycle (EUDC) [26] and acceleration test, with the same base model and control rule. EUDC is a driving cycle that was established by the European Union. EUDC is designed to assess the emission levels of car engines and fuel economy in passenger cars, which excludes light trucks and commercial vehicles.

3.1. Extra-Urban Driving Cycle

The EUDC is designed to represent more aggressive, high-speed driving conditions, as shown in Figure 12a. The maximum speed of the EUDC is 120 km/h, starting from the still phase. In this driving condition, the functions of an idle start in the EV mode and power assist for high power demand are enabled. Figure 12b shows the simulation results of the following EUDC with different k_2 values and the same overall gear ratio. Figure 12c shows the engine on–off state. Figure 12c shows that the engine is always on under the EUDC, excluding the start-from-still phase and the brake-to-still phase. Figure 12d shows that the EM is also on in the 316–336th second regions, excluding the start-from-still and brake-to-still phase. Table 6 shows fuel consumption under the EUDC with different k_2 values. The optimal results are obtained for $k_2 = 1.6$, wherein fuel consumption improves by 1.5%, because the vehicle can be driven for a longer duration in the EV mode and the required torque can be provided in the hybrid mode. The detailed effects of k_2 values are discussed in the following discussions.

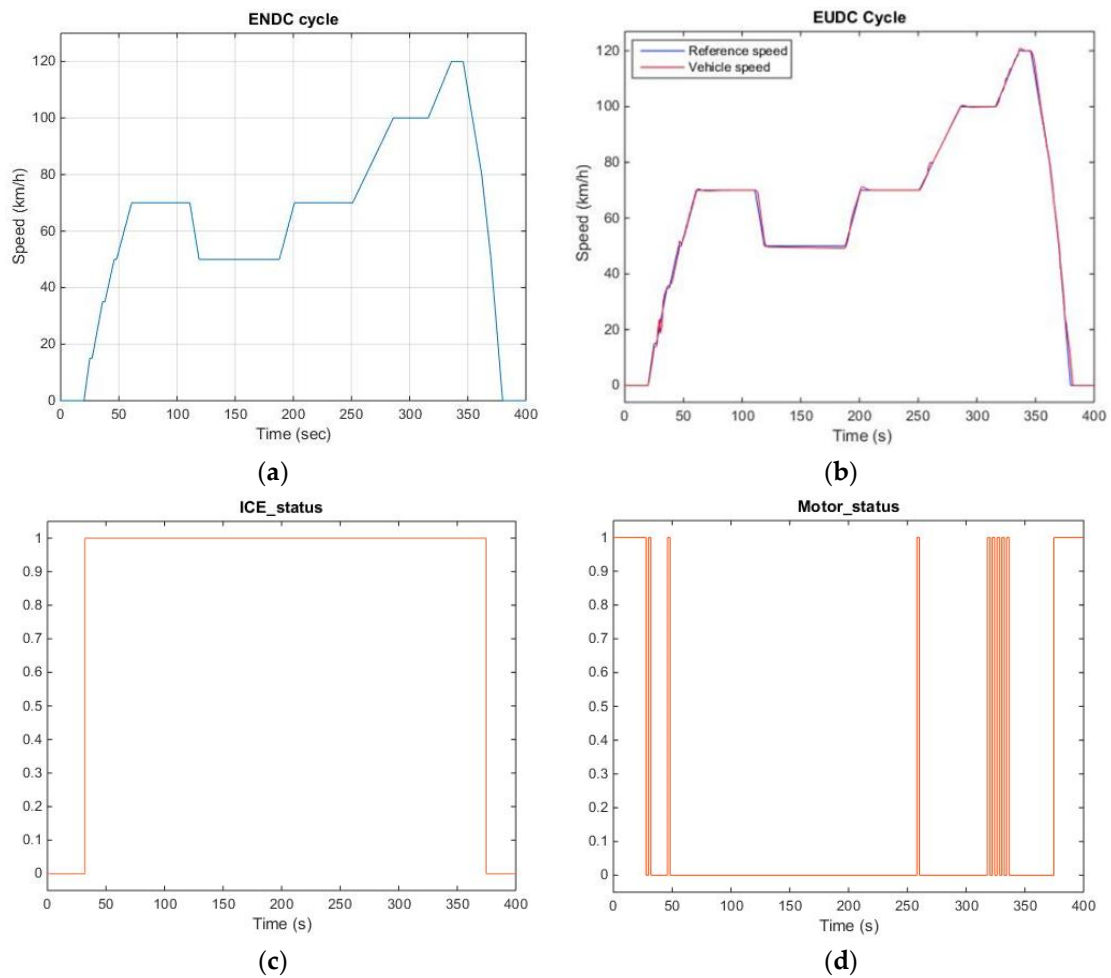


Figure 12. (a) Standard extra-urban driving cycle (EUDC) driving cycle. (b) Simulation follow driving cycle. (c) Status of engine. (d) State of motor ($k_2 = 1$).

Table 6. Fuel consumption under extra-urban driving cycle (EUDC).

	$k_2 = 1$	$k_2 = 1.2$	$k_2 = 1.4912$	$k_2 = 1.6$
EV gear ratio	19.92	14.06	13.36	12.45
EV overall ratio			19.92	
Fuel consumption (km/L)	16.9	16.98	17.12	17.15

Figure 13a shows the different motor statuses, which indicate that a larger k_2 value drives the motor for a longer duration in the EV mode. Figure 13b shows the motor torque that is provided under the EUDC. The motor provides a positive torque under the EUDC, which indicates that the motor works as a traction motor. Engage and disengage clutches when shifting the gear or when changing the driving mode generate negative impulse. Figure 13c shows that the motor provides a torque in the power-assist region, and a smaller of k_2 value provides more torque, whereas a larger k_2 provides less torque from the motor side before TC-PIM. The torque that is provided by the motor increases after the 325th second due to gear shifting, as shown in Figure 13d. Table 7 shows that the torque provided by the motor after the TC-PIM is larger for $k_2 = 1.6$; thus, higher k_2 values exhibit superior power-assist ability.

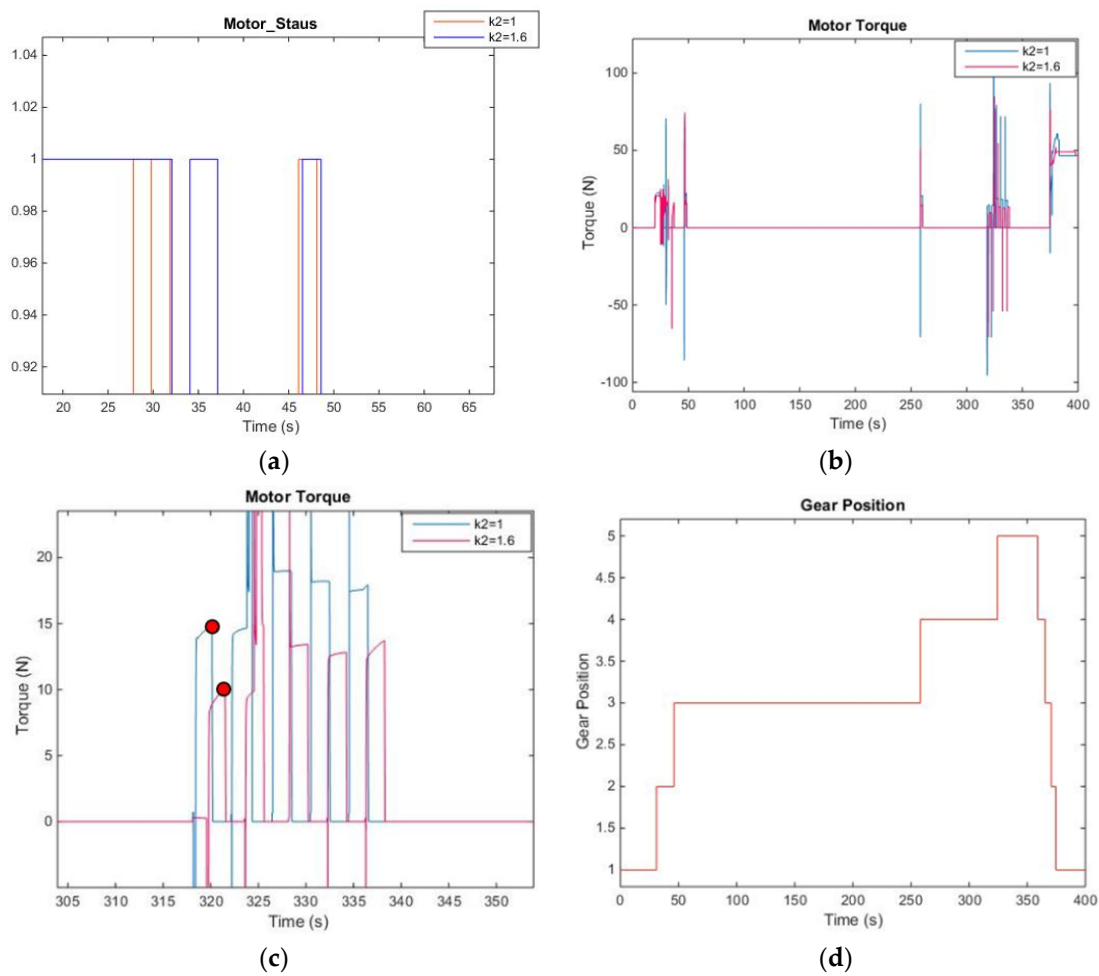


Figure 13. (a) Comparison of motor status. (b) Comparison of motor torque. (c) Comparison of motor torque at power-assist region. (d) Gear position.

Table 7. Simulated torque convert values.

	$k_2 = 1$	$k_2 = 1.6$
Torque (Nm)	14.85	10.07
Torque after TC-PIM (Nm)	14.85	16.112

Figure 14a presents the reason why larger k_2 values cause a longer driving time in the EV mode. Due to the EV gear ratio and k_2 being different, the required speed and TW speed are different when the speed of the drive shaft placed before the gearbox is more than 3000 rpm. For a larger k_2 value, the vehicle can operate the motor in the higher speed region and drive the vehicle with higher speed in the EV mode. Therefore, the vehicle can drive for a longer duration in the EV mode. Figure 14b shows why the motor provides torque before the TC-PIM. Larger k_2 values can provide lower torque to reach the load demand because of the fixed load and fixed gear ratio.

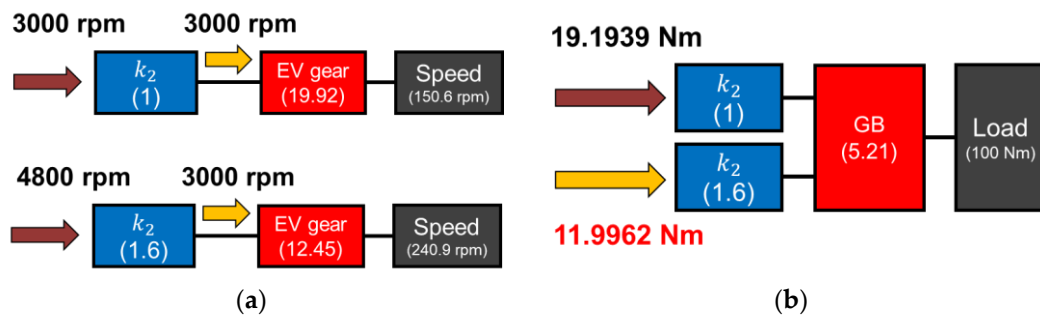


Figure 14. (a) Influence of different k_2 and electric vehicle (EV) gear ratio and (b) influence of torque applies with different values k_2 .

Figure 15a–d present the operation points of the engine under the EUDC. The engine starts at approximately 3000 rpm to avoid an idle start, and many operation points are observed between the 3000-rpm and 5000-rpm region because of gear shifting for controlling the engine speed in this region.

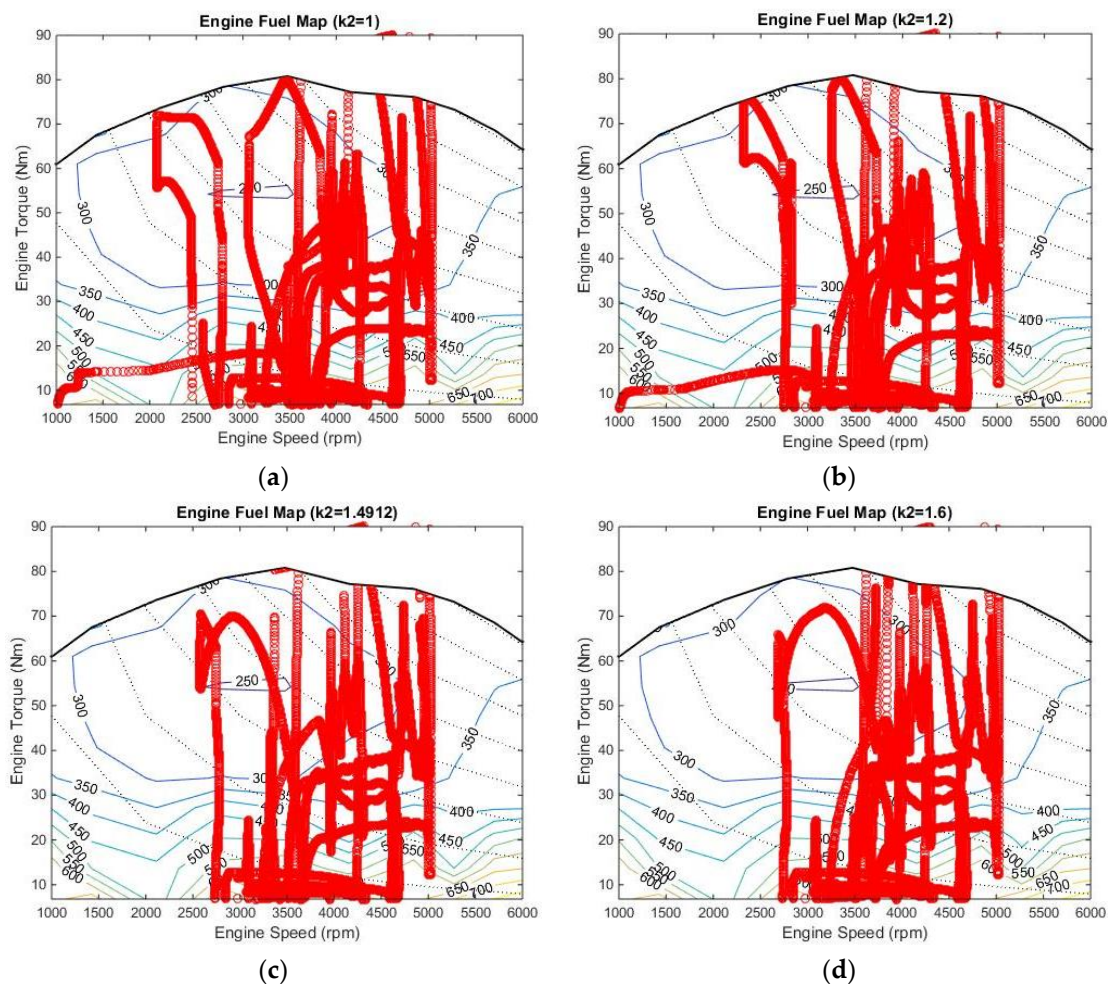


Figure 15. (a) Engine operation points (with $k_2 = 1$). (b) Engine operation fuel points (with $k_2 = 1.2$). (c) Engine operation points (with $k_2 = 1.4912$). (d) Engine operation points (with $k_2 = 1.6$).

Figure 16a–d provide the operation points of the motor under the EUDC with different k_2 values. The operation points are evident in different regions as the k_2 values change.

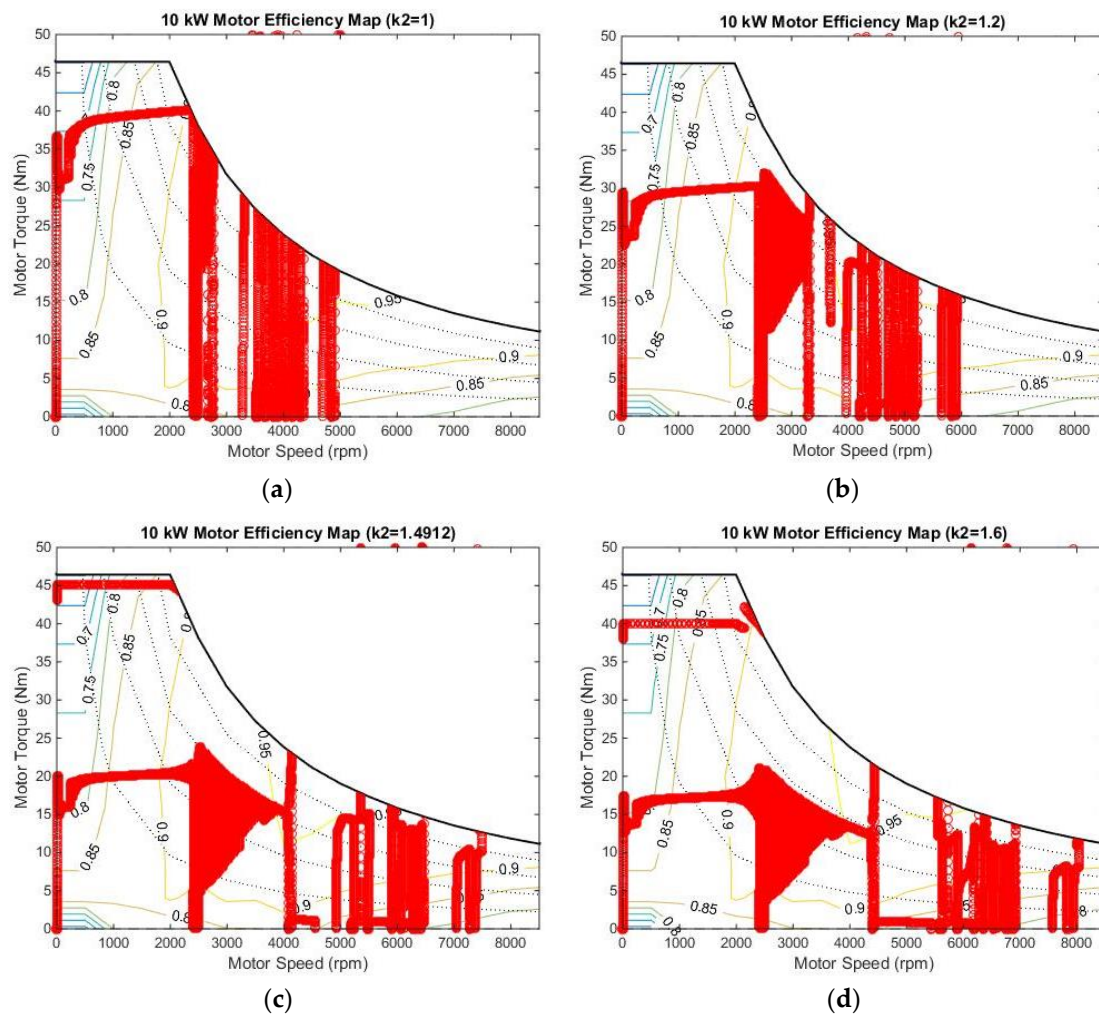


Figure 16. (a) Motor operation points (with $k_2 = 1$). (b) Motor operation points (with $k_2 = 1.2$). (c) Motor operation points (with $k_2 = 1.4912$). (d) Motor operation points (with $k_2 = 1.6$).

3.2. Top Speed and Acceleration Test

Figure 17 shows that, in both 0–60 km/h and 0–100 km/h acceleration tests, smaller k_2 values provide improved acceleration ability. Figure 17a presents the acceleration test results from the start to the top speed without the top speed gear. Table 8 reveals that differences in k_2 values did not influence the top speed, because the fourth gear is designed for the engine-only mode. Although the propulsion system can provide excess torque in the hybrid mode, the maximum vehicle speed is limited by the TW speed, which the gear ratio of the fourth gear constrained. Figure 17b presents the acceleration test results from the start to the top speed with the top speed gear. The top speed at $k_2 = 1$, $k_2 = 1.2$, and $k_2 = 1.4912$ are almost the same, but they are slightly lower than the ideal maximum speed, which is the speed of engine at maximum power condition in hybrid mode. The top speed at $k_2 = 1.6$ is lower than that at other k_2 values, because the rotation speed before the gearbox is limited by the motor speed after the TC-PIM at $k_2 = 1.6$. The maximum speed in the hybrid mode is lower than the maximum rotational speed of the engine under the maximum power condition. Although the propulsion system can provide excess torque to overcome the total resistance, the maximum vehicle speed is lower than the ideal maximum speed. The difference between the top speed at $k_2 = 1.6$ and other k_2 values is approximately 11.59 km/h, which validates that an inappropriate k_{ratio} design influences the top speed of the TC-type parallel hybrid vehicle.

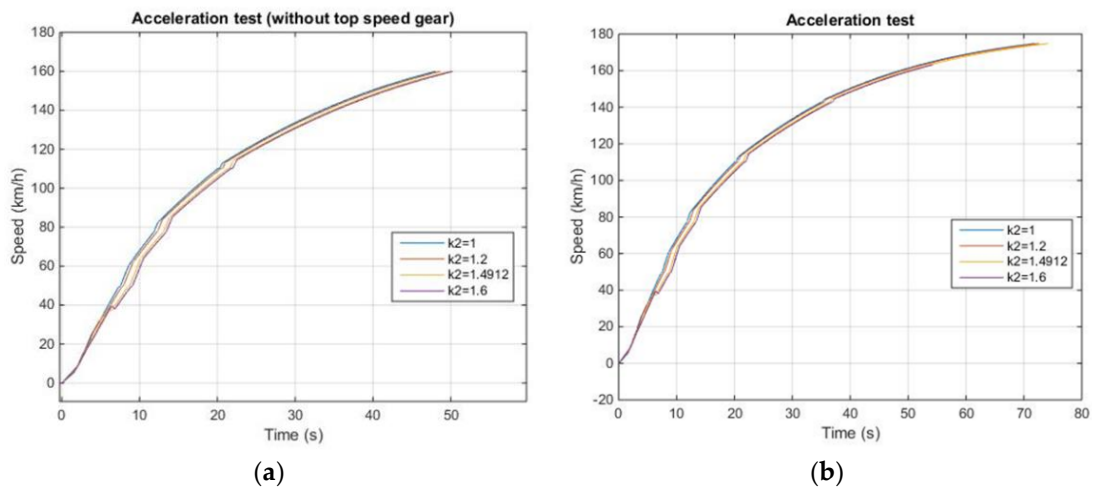


Figure 17. (a) Acceleration test with different k_2 values without top speed gear. (b) Acceleration test under different k_2 values with top speed gear.

Table 8. Top speed result and acceleration time with different k_2 values.

	$k_2 = 1$	$k_2 = 1.2$	$k_2 = 1.4912$	$k_2 = 1.6$
Top speed without top speed gear (km/h)	159.95	159.95	159.95	159.95
Top speed (km/h)	174.83	174.84	174.84	163.25
0–60 km/h acceleration time (s)	8.57	8.95	9.74	10.11
0–60 km/h acceleration time gap (s)		0.38	1.17	1.54
0–100 km/h acceleration time (s)	17.08	17.37	18.15	18.5
0–100 km/h acceleration time gap (s)		0.29	1.07	1.42

Figure 18a and Table 8 show the acceleration times for 0–60 km/h and 0–100 km/h under different k_2 values. However, after the start motion, larger k_2 values have improved acceleration ability than smaller k_2 values. Figure 18b shows the change in the driving mode from the EV mode to the ICE mode. In this phase, smaller k_2 values exhibit deteriorating acceleration ability due to torque loss from engine pumping loss.

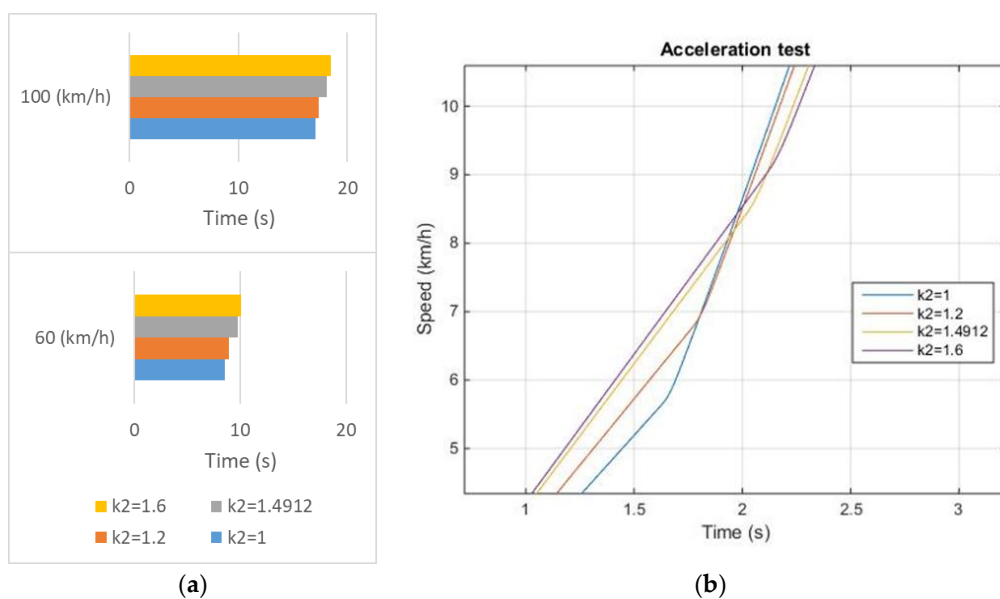


Figure 18. (a) Acceleration time compared with different k_2 values. (b) Acceleration in mode change phase (EV to ICE).

Figure 19a shows engine pumping loss under the EUDC test and, thus, the motor provides a torque to TWs and to start the rotation of the engine. Figure 19b shows the influence of engine pumping loss on the pre-transmission architecture. As the engine pumping loss is almost constant, the torque after the TC-PIM is affected. When the k_2 value is larger, the torque after the TC-PIM is larger. The engine pumping loss requires a smaller percentage of the total value of the torque after the TC-PIM and, thus, the acceleration ability is superior for larger k_2 values in the EV mode. However, when the driving mode changes from the EV mode to ICE mode, the acceleration ability rapidly increases because the engine can provide a larger torque than the EM. Smaller k_2 values enable an earlier change in the driving mode from the EV mode to the ICE mode. This observation is because smaller k_2 values exhibit more improved acceleration ability. Apart from the mode change, Table 8 shows that the time gap between each k_2 value and the smallest k_2 value improves. Larger k_2 values can improve the time gap, which indicates that larger k_2 values have more improved superior power-assist ability. This result is consistent with that of the EUDC test.

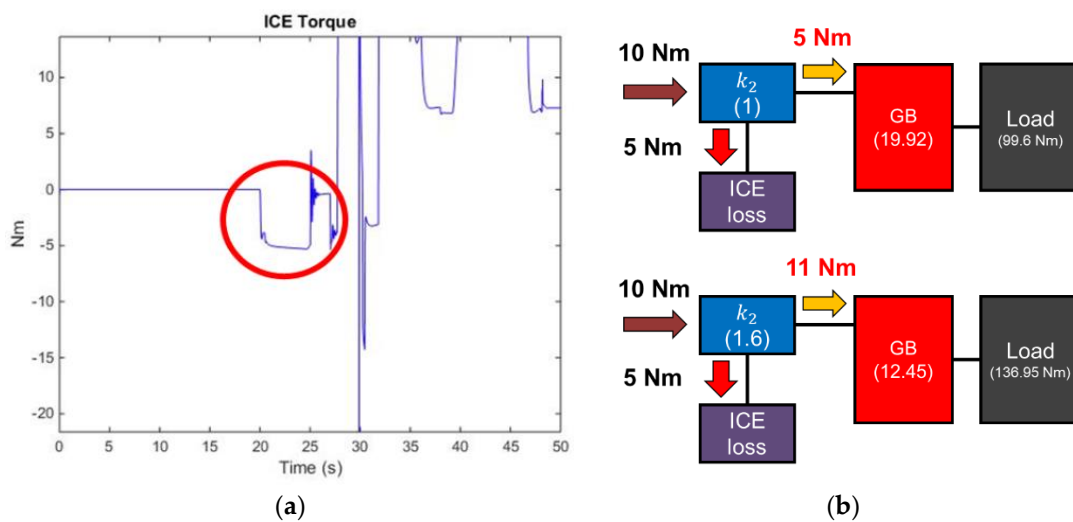


Figure 19. (a) Engine pumping loss. (b) Pumping loss inference in pre-transmission architecture.

4. Discussion

The design of the parallel hybrid transmission system is different from that of the single power transmission system. Apart from the design gear ratio for driving requirements, the k_{ratio} in the PIM is the most crucial factor for the efficient and smooth combination of the engine and EM. For TC-PIM-type parallel hybrid transmission, the k_{ratio} can be designed by comparing the speed range of two power units with any ratio; however, the maximum ideal k_{ratio} must be exceeded. The other design focuses on selecting the location of the gearbox at the parallel hybrid driveline. The study presents the principle for selecting the transmission architecture for the parallel hybrid vehicle. For the TC-type parallel hybrid vehicle, η_{speed} can be used to determine the transmission architecture. We implement the pre-transmission architecture and determine the effect of this transmission architecture. The effects of the gear ratio design for the pre-transmission architecture are as follows:

1. The EV mode gear ratio must be designed, which influences the top speed of the EV mode.
2. To improve the top speed ability, a top speed gear is must be designed. In this study, the top speed ability in the hybrid mode is improved by approximately 9.3%.

The influences of the k_{ratio} with the fixed overall gear ratio for the pre-transmission system are as follows:

1. A higher k_{ratio} has more improved power-assist ability. In this study, a k_{ratio} of 1.6 improves the power-assist ability by approximately 8.5% when compared with the k_{ratio} of 1.

2. The higher k_{ratio} provides wider-speed-region operation.
3. A higher k_{ratio} can reduce the influence of engine pumping loss and, thus, it has more improved acceleration ability in the EV mode.
4. The top speed performance decreases with an improper k_{ratio} , which exceeds the maximum ideal k_{ratio} . In this study, the top speed at the k_{ratio} of 1.6 is lower by approximately 6.63% than the top speed at a k_{ratio} of 1.

Apart from the k_{ratio} , the torque–speed characteristic and hybridization factor are crucial in the smooth coordination of the two power units in the hybrid power system. The relationship between the k_{ratio} and torque–speed characteristics is unclear. The quality of the design principle the k_{ratio} combined with the torque–speed characteristic must be examined. Apart from the TC-PIM, another power integral speed-coupled mechanism is available. The design principle of the k_{ratio} for the SC-PIM must be determined in the future. Therefore, a more efficient and powerful hybrid vehicle can be designed.

5. Conclusions

The design of TC-PIM parameters (i.e., k_1 and k_2) are based on k_{ratio} theory. We can uncover effective k values for TC-PIM and a suitable location of gearbox, by following the simulations of driving cycles (EUDC) and acceleration test. The results show that a higher k_{ratio} has more improved power-assist ability for the pre-transmission architecture. For example, the k_{ratio} of 1.6 can improve the power-assist ability by 8.5% as compared with the k_{ratio} of 1. In the design with an appropriate gear ratio and k_{ratio} , the top speed ability of the vehicle can be improved by 9.3%, whereas, in an improper design, the top speed ability of vehicle can be improved by 2.06%. The simulation results show that the transmission system design influences vehicle performance, and it uses the combined power of the two power units for the parallel hybrid vehicle. The design matching principle that is proposed in this study can determine the effective design range of the TC-PIM parameters and gear ratio of the gearbox. It can be used as a design reference theory for the transmission system of parallel hybrid vehicles. However, performing the tests for practical vehicles remains challenge due to the difficulties of the experimental constructions, including power integration mechanism, power units, gearbox, etc. The practical experiments may be demonstrated as future works.

Author Contributions: Conceptualization, P.-H.P.; methodology, P.-H.P.; software, P.-H.P.; validation, P.-T.C., P.-H.P. and K.D.H.; formal analysis, P.-H.P.; investigation, P.-H.P.; resources, C.-J.Y.; data curation, P.-H.P.; writing—original draft preparation, P.-T.C. and C.-J.Y.; writing—review and editing, P.-T.C. and C.-J.Y.; visualization, P.-H.P.; supervision, C.-J.Y. and K.D.H.

Funding: This research received no external funding.

Acknowledgments: P.-T.C. thank the financial supported from the Center of Atomic Initiative for New Materials (AI-Mat), National Taiwan University, Taipei, Taiwan from the Featured Areas Research Center Program within the framework of the Higher Education Sprout Project by the Ministry of Education (MOE) in Taiwan. This manuscript was edited by Wallace Academic Editing.

Conflicts of Interest: The authors declare no conflict of interest.

Appendix A Nomenclature (Including Subscript)

A	Front area of vehicle body (m^2)
C_d	Drag coefficient
C_g	Mass center of vehicle
F_D	Drag resistance (N)
F_G	Grade resistance (N)
F_{Gmax}	Maximum grade resistance (N)
F_R	Rolling resistance (N)
F_T	Traction force (N)

P_{max}	Maximum power of power units (kW)
N	Normal force of tire (N)
T_1	Torque of port 1 (Nm)
T_2	Torque of port 2 (Nm)
T_3	Torque of port 3 (Nm)
T_d	Torque of drive gear (Nm)
T_{dn}	Torque of driven gear (Nm)
T_w	Torque of traction wheel (Nm)
T_{max}	Maximum torque of power units (Nm)
V_{max}	Maximum vehicle speed (m/s)
a	Acceleration speed (m/s ²)
d	Tiny offset of wheel center (m)
f_R	Rolling resistance coefficient
i_{EV}	Gear ratio of EV mode
$i_{Hy-smallest}$	The smallest gear ratio of hybrid mode
$i_{ICE-largest}$	The largest gear ratio of ICE mode
$i_{ICE-smallest}$	The smallest gear ratio of ICE mode
$i_{largest}$	The largest gear ratio
i_n	Gear ratio of n gear
$i_{overall}$	Overall gear ratio of transmission
$i_{smallest}$	The smallest gear ratio
k_1	Gear ratio of port 1
k_2	Gear ratio of port 2
k_{ratio}	Ratio of k_1 and k_2
k_{ratio_max}	Ideal maximum ratio of k_1 and k_2
m	Mass of vehicle (kg)
m^*	Inertia mass of vehicle (kg)
n_{max}	Maximum speed of power units at maximum power condition (rpm)
n_{Tmax}	Speed of power units at maximum torque (rpm)
r_d	Radius of drive gear (m)
r_{dn}	Radius of driven gear (m)
r_{weff}	Effective radius of traction wheel (m)
v	Vehicle speed (m/s)
ω_1	Angular velocity of port 1 (rad/s)
ω_{1-Pmax}	Angular velocity of port 1 at maximum power condition (rad/s)
ω_2	Angular velocity of port 2 (rad/s)
ω_{2-Pmax}	Angular velocity of port 2 at maximum power condition (rad/s)
ω_3	Angular velocity of port 3 (rad/s)
ω_{3-Pmax}	Angular velocity of port 3 at maximum power condition (rad/s)
ω_d	Angular velocity of drive gear (rad/s)
ω_{dn}	Angular velocity of driven gear (rad/s)
ω_{E-max}	Maximum speed of electric motor (rpm)
$\omega_{ICE-max}$	Maximum speed of engine (rpm)
θ	Angle of slope
η	Efficiency of gear train
η_{speed}	Speed ratio after TC-PIM
φ	Gear step
φ_1	Progressive typical values
φ_2	Selected progressive factor
ρ	Air density (kg/m ³)

Abbreviations

EM	Electric moter
EV	Electric vehicle
EUDC	Extra-urban driving cycle
FUDS	Federal urban driving cycle
GB	Gearbox
ICE	Internal combustion engine
PID	Proportional integral derivative
PIM	Power integration mechanism
PMDC	Permanent magnet direct current
SI	Spark ignition
TC-PIM	Torque-coupled-type power integration mechanism
TW	Traction wheel

References

- Samadani, E.; Farhad, S.; Panchal, S.; Fraser, R.; Fowler, M. Modeling and Evaluation of Li-Ion Battery Performance Based on the Electric Vehicle Field Tests. *SAE Technical Paper Series*. 2014, 2014-01-1848. Available online: <https://doi.org/10.4271/2014-01-1848> (accessed on 11 April 2019). [CrossRef]
- Panchal, S.; Mathew, M.; Dincer, I.; Agelin-Chaab, M.; Fraser, R.; Fowler, M. Thermal and electrical performance assessments of lithium-ion battery modules for an electric vehicle under actual drive cycles. *Electr. Syst. Res.* **2018**, *163*, 18–27. [CrossRef]
- Chen, P.-T.; Yang, F.-H.; Sangeetha, T.; Gao, H.-M.; Huang, K.D. Moderate Energy for Charging Li-Ion Batteries Determined by First-Principles Calculations. *Batter. Supercaps* **2018**, *1*, 209–214. [CrossRef]
- Chen, P.T.; Yang, F.H.; Cao, Z.T.; Jhang, J.M.; Gao, H.M.; Yang, M.H.; Huang, K.D. Reviving Aged Lithium-Ion Batteries and Prolonging Their Cycle Life by Sinusoidal Waveform Charging Strategy. *Batter. Supercaps* **2019**, accepted. [CrossRef]
- Huang, K.D.; Sangeetha, T.; Cheng, W.-F.; Lin, C.; Chen, P.-T. Computational Fluid Dynamics Approach for Performance Prediction in a Zinc–Air Fuel Cell. *Energies* **2018**, *11*, 2185. [CrossRef]
- Sangeetha, T.; Chen, P.-T.; Cheng, W.-F.; Yan, W.-M.; Huang, K.D. Optimization of the Electrolyte Parameters and Components in Zinc Particle Fuel Cells. *Energies* **2019**, *12*, 1090. [CrossRef]
- Min, H.; Lai, C.; Yu, Y.; Zhu, T.; Zhang, C. Comparison Study of Two Semi-Active Hybrid Energy Storage Systems for Hybrid Electric Vehicle Applications and Their Experimental Validation. *Energies* **2017**, *10*, 279. [CrossRef]
- Wellesley Toyota, How Your Toyota Hybrid Engine Works? Available online: <http://blog.wellesleytoyota.com/blog/bid/328878/How-Your-Toyota-Hybrid-Engine-Works> (accessed on 1 June 2018).
- Xiao, R.; Liu, B.; Shen, J.; Guo, N.; Yan, W.; Chen, Z. Comparisons of Energy Management Methods for a Parallel Plug-In Hybrid Electric Vehicle between the Convex Optimization and Dynamic Programming. *Appl. Sci.* **2018**, *8*, 218. [CrossRef]
- Kim, H.; Wi, J.; Yoo, J.; Son, H.; Park, C.; Kim, H. A Study on the Fuel Economy Potential of Parallel and Power Split Type Hybrid Electric Vehicles. *Energies* **2018**, *11*, 2103. [CrossRef]
- Lukic, S.; Emadi, A. Effects of Drivetrain Hybridization on Fuel Economy and Dynamic Performance of Parallel Hybrid Electric Vehicles. *IEEE Trans. Veh. Technol.* **2004**, *53*, 385–389. [CrossRef]
- Lukic, S.; Cao, J.; Bansal, R.; Rodriguez, F.; Emadi, A. Energy Storage Systems for Automotive Applications. *IEEE Trans. Ind. Electron.* **2008**, *55*, 2258–2267. [CrossRef]
- Miller, J.M. *Propulsion System for Hybrid Vehicles*, 2nd ed.; IET Digital Library: London, UK, 2011; pp. 62–81, ISBN 978-1-84919-147-0.
- Zulkifli, S.A.; Saad, N.; Aziz, A.R.A.; Ghani, S.C.; Alias, A.; Mamat, R.; Rahman, M.M. Comparative Analysis of Torque and Acceleration of Pre- and Post-Transmission Parallel Hybrid Drivetrains. *MATEC Web Conf.* **2016**, *74*, 1. [CrossRef]
- Hoang, N.-T.; Yan, H.-S. Configuration Synthesis of Novel Series-Parallel Hybrid Transmission Systems with Eight-Bar Mechanisms. *Energies* **2017**, *10*, 1044. [CrossRef]

16. Bonfiglio, A.; Lanzarotto, D.; Marchesoni, M.; Passalacqua, M.; Procopio, R.; Repetto, M. Electrical-Loss Analysis of Power-Split Hybrid Electric Vehicles. *Energies* **2017**, *10*, 2142. [CrossRef]
17. Zhang, X.; Li, C.T.; Kum, D.; Peng, H. Prius+ and Volt–: Configuration Analysis of Power-Split Hybrid Vehicles with a Single Planetary Gear. *IEEE Trans. Veh. Technol.* **2012**, *61*, 3544–3552. [CrossRef]
18. Fischer, R.; Küçükay, F.; Jürgens, G.; Najork, R.; Pollak, B. *The Automotive Transmission Book*, 2015th ed.; Springer: Cham, Switzerland, 2015; ISBN 978-3319052625.
19. Cossalter, V. *Motorcycle Dynamics*, 2nd ed.; LuLu Enterprises, Inc.: Morrisville, NC, USA, 2006; ISBN 978-1-4303-0861-4.
20. Naunheimer, H.; Bertsche, B.; Ryborz, J.; Novak, W. *Automotive Transmissions*, 2nd ed.; Springer: Cham, Switzerland, 2011; pp. 102–113, ISBN 978-3-642-16214-5.
21. Ehsani, M.; Gao, Y.; Emadi, A. *Modern Electric, Hybrid Electric, and Fuel Cell Vehicles: Fundamentals, Theory, and Design*, 2nd ed.; CRC Press: Boca Raton, FL, USA, 2009; pp. 112–120, ISBN 978-1420053982.
22. Lin, C.-C.; Peng, H.; Grizzle, J.W.; Kang, J.-M. Power management strategy for a parallel hybrid electric truck. *IEEE Trans. Control Syst. Technol.* **2003**, *11*, 839–849.
23. Matlab Simulink of ADVISOR® Software and Advanced Vehicle Simulator. Available online: <https://sourceforge.net/projects/adv-vehicle-sim> (accessed on 12 March 2019).
24. *Simscape User's Guide*, R2018b ed.; The MathWorks Inc.: Natick, MA, USA, 2018.
25. *Simscape Driveline User's Guide*, R2018b ed.; The MathWorks Inc.: Natick, MA, USA, 2018.
26. ECE15+ EUDC/NEDC. Emission Test Cycles. Available online: https://www.dieselnet.com/standards/cycles/ece_eudc.php (accessed on 12 March 2019).



© 2019 by the authors. Licensee MDPI, Basel, Switzerland. This article is an open access article distributed under the terms and conditions of the Creative Commons Attribution (CC BY) license (<http://creativecommons.org/licenses/by/4.0/>).